$$\frac{E(\gamma_i)}{\gamma_i} = E(P)/P + [E(T)/p_i^\circ]\,[dp_i^\circ/dT] + [(1/y_i) + (1/x_i)]\,E(x) \quad (8)$$

$$E(Q) = \sum_i \left[x_i \frac{E(\gamma_i)}{\gamma_i} + E(x) \ln \gamma_i \right] \quad (9)$$

$$E(\alpha_1) = \frac{E(\gamma_1)}{\gamma_1} - \frac{E(\gamma_2)}{\gamma_2} \quad (10)$$

The maximum errors of measurement are $E(T) = 0.05$, $E(P) = 0.5$, and $E(x) = 0.01$. The values of α_{1_e} are plotted against x_i in Figure 3 along with the noise bounds and calculated α_{1_c}. This figure shows that calculated values of thermodynamic functions α_1 are within the noise bounds which indicates local as well as over-all consistency of the data.

The thermodynamic consistency of the data was also tested using Chao's (*1*) modified Redlich-Kister equation. The values of constants in the equation,

$$\log \frac{\gamma_1}{\gamma_2} = a + b(x_2 - x_1) + c(6x_1x_2 - 1) + d(x_2 - x_1)\,(1 - 8x_1x_2) \quad (11)$$

are $a = 0.048$, $b = 0.730$, $c = 0.096$, and $d = 0.130$.

The area test of Redlich-Kister (*5*) is satisfactory, and the calculated values of log γ_1/γ_2 from Equation 11 are in good agreement with experimental values. Herington's test (*4*) for consistency is also satisfactory since experimental $D\text{-}J = 4.74 < 10$.

NOMENCLATURE

- a, b, c, d = constants in Chao's equation
- A, B = defined functions in Equation 5
- E = error
- H = integral heat of mixing
- P = total pressure
- p° = vapor pressure of pure component
- Q = dimensionless excess free energy
- R = gas constant
- T = absolute temperature
- V = integral volume change of mixing
- x = mole fraction of component in liquid phase
- y = mole fraction of component in vapor phase
- γ_1 = dimensionless thermodynamic function in Equations 5 and 7
- γ = liquid activity coefficient
- θ_i = vapor imperfection coefficient

Subscripts

- r, s = points on a linear path
- i = component identity
- c = computed indirectly from data
- e = computed directly from experimental results
- 1 = *n*-heptane
- 2 = *n*-butanol

LITERATURE CITED

(1) Chao, K.C., Hougen, O.A., *Chem. Eng. Sci.* **7**, 246 (1958).
(2) Ellis, S.R.M., Garbett, R.D., *Ind. Eng. Chem.* **52**, 385 (1960).
(3) "Handbook of Chemistry and Physics," 44th ed., Charles D. Hodgman, Ed., Chemical Rubber Publishing Co., Cleveland, Ohio, 1962–63.
(4) Herington, E.F.G., *J. Inst. Petrol.* **37**, 457 (1951).
(5) Redlich, O., Kister, A.T., *Ind. Eng. Chem.* **40**, 345 (1948).
(6) Smyth, C.P., Engel, E.W., *J. Am. Chem. Soc.* **51**, 2660 (1929).
(7) Tao, L.C., *Ind. Eng. Chem.* **56**, 36 (1964).
(8) Vijayaraghavan, S.V., Deshpande, P.K., Kuloor, N.R., *Indian J. Tech.* **2**, 249 (1964).

RECEIVED for review October 5, 1964. Accepted February 9, 1966.

Transient Solute Concentrations and Phase Changes of Calcium Sulfate in Aqueous Sodium Chloride

WILSON H. POWER and BELA M. FABUSS
Monsanto Research Corporation, Everett, Mass.

CHARLES N. SATTERFIELD
Massachusetts Institute of Technology, Cambridge, Mass.

The change in solute concentration with time of 0.25*m* or 1.0*m* NaCl in contact with gypsum, β-hemihydrate, β-soluble anhydrite, or insoluble anhydrite was determined over the temperature range of 25° to 105° C. Accompanying changes in the solid phase were also determined. Under thermodynamically favorable conditions, β-hemihydrate and β-soluble anhydrite rapidly hydrate to form gypsum. The dehydration rate of gypsum at 95° and 105° C. to form insoluble anhydrite is much faster in 1.0*m* NaCl than in pure water. Some changes in solubility and solid phase composition occur only after an induction period of 2 days or more. Solubility product constants for gypsum and insoluble anhydrite agree closely with previously published values. From present data and earlier literature values, a correlation is presented for estimating the solubility of gypsum and anhydrite over a wide range of ionic strength.

AN EARLIER PAPER (*7*) reported on the change in solute concentration of water with time in contact with α- or β-calcium sulfate hemihydrate, β-soluble anhydrite, or insoluble anhydrite. The changes in solute concentration were related to changes in the nature of the calcium sulfate solid phase present. The present study extends the earlier work to an investigation of the transient behavior of various forms of calcium sulfate in contact with aqueous sodium chloride solutions.

Measurements were carried out in a 1-liter borosilicate glass flask, and the experimental method was as previously described except that in the presence of sodium chloride, conductivity could not be used to determine calcium sulfate solubility as before. Instead, solutions were analyzed for

calcium by the (ethylenedinitrilo) tetraacetic acid (EDTA) method used previously. X-ray diffraction examinations of solid specimens were made with a General Electric Diffractometer XRD-3 with a nickel filter.

Studies were made with gypsum ($CaSO_4 \cdot 2H_2O$), β-hemihydrate (β-$CaSO_4 \cdot \frac{1}{2} H_2O$), β-soluble anhydrite (β-$CaSO_4$), and insoluble anhydrite at temperatures from 25° to 105° C. in either 0.25*m* or 1.0*m* NaCl aqueous solution. The modifications of calcium sulfate were prepared in the same way as those used and described previously (7). The gypsum crystals were in the form of elongated prisms about 2 × 10 microns on the average. The salt was slurried with water and filtered before being used for solubility measurements. The total water content (free and as hydrate) of the gypsum filter cake was approximately 50%.

RESULTS

Over the range of conditions used here, the solubility of all modifications of calcium sulfate increases with sodium chloride concentration. However, gypsum and the hemihydrate were converted to insoluble anhydrite much more readily in contact with a sodium chloride solution than in contact with water. In the presence of water, gypsum is the thermodynamically stable solid phase only at temperatures below 40° to 41° C. (7, Figure 1). Above this temperature, insoluble anhydrite is the thermodynamically stable phase, but if one starts with gypsum in contact with pure liquid water, the rate of phase transformation to insoluble anhydrite is extremely slow. In the previous studies with water over the temperature range of 25° to 100° C., the characteristic solubility of gypsum was obtained within a fraction of a minute after the salt was agitated with pure water, and analyses of the solid phase consistently indicated the presence of only the dihydrate at all temperatures in this range and at all contact times studied—up to 222 hours. If the difficult-to-obtain insoluble anhydrite phase is neglected, then a meta-stable equilibrium point between gypsum, α-hemihydrate, and liquid water exists at about 99° C., and another equilibrium point between gypsum, β-hemihydrate, and liquid water exists at about 103° C. Above 103° C., the meta-stable phase is a hemihydrate and below 99° C. it is gypsum.

Gypsum. In contact with 1*m* sodium chloride, the calcium sulfate solute concentration equaled the solubility of gypsum over the entire period studied (up to 120 hours) at temperatures of 85° C. or lower. The hydrate water content of the solid remained constant at the stoichiometric value of 20.9%. At 95° C., however, as shown on Figure 1, top, the calcium sulfate concentration equaled the gypsum solubility for about the first 60 hours and then slowly decreased to approach the solubility of insoluble anhydrite in 1*m* sodium chloride. Simultaneously, the hydrate water content of the solid phase remained equal to that of gypsum for about the first 50 hours and then decreased to less than 1%. X-ray diffraction analysis of the final solid phase showed it to be insoluble anhydrite. At 105° C., both the calcium sulfate concentration and hydrated water content of the solid phase rapidly decreased immediately after the initial contact of gypsum with the 1*m* salt solution. These results are in strong contrast to the behavior of gypsum in water, where at 100° C. no change in water content of the solid phase or solute content was observed over a 72-hour period. Table I presents the data on the solubility of gypsum in water, 0.25*m* sodium chloride, and 1.0*m* sodium chloride over the range of 25° to 95° C. The value for 95° C. and 1.0*m* NaCl is for the early flat portion of the curve before dehydration occurred.

β-Hemihydrate. Both β-hemihydrate and β-soluble anhydrite are more soluble than gypsum in water up to the transition temperature of 97° to 99° C. and are unstable modifications at lower temperatures, being rapidly converted to gypsum. When added to water, the solute content rises rapidly up to a maximum after a few minutes and then decreases to a limiting value equal to that for gypsum.

In 1*m* sodium chloride, the same phenomenon occurs, except that, with the present experimental procedure, the

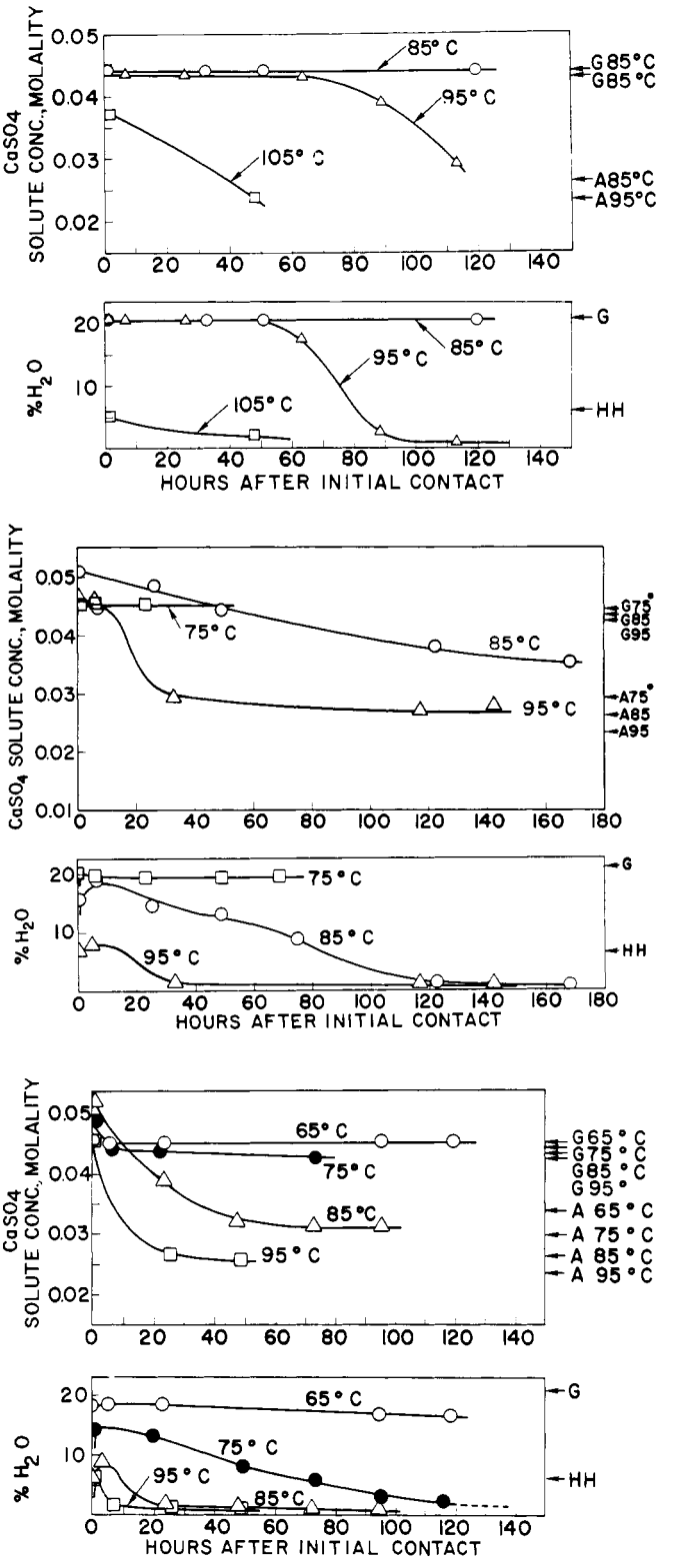

Figure 1. Transient solute concentration and hydrate water content of solid phase upon contacting gypsum (top), β-hemihydrate (middle), and β-soluble anhydrite (bottom) with 1*m* sodium chloride

Arrows on right-hand ordinate indicate salubility (at specified temperature) or water content of gypsum (G), anhydrite (A), or hemihydrate (HH)

details of the first few minutes' rise to a maximum and subsequent drop could not be followed. At temperatures below 75° C., the calcium sulfate concentration rapidly decreases to that of gypsum as hydration occurs, and the solid rapidly acquires the dihydrate composition. At 75° C., the solute concentration was essentially constant at 0.0452*m* $CaSO_4$ for up to 23 hours, and the solid composition stayed constant at 19.5% H_2O, slightly less than that of the dihydrate, for 69 hours. At 85° C., as shown on Figure 1, middle, the initial transient high calcium sulfate concentration is prolonged for several hours before decreasing to equal the solubility of gypsum. After about 70 hours, however, the calcium sulfate concentration gradually decreases further, below the solubility of gypsum. Accompanying these solute concentration changes, the hydrate water content of β-hemihydrate rises sharply after contact with 1*m* sodium chloride to approach, but not quite attain, the dihydrate composition. After reaching this maximum—at about 5 hours contact time—the hydrate water content of the solid phase gradually decreases until it is less than 1% after 150 hours contact time. At 95° C., after bringing β-hemihydrate into contact with sodium chloride solution, the calcium sulfate solute concentration decreases rapidly to approach the solubility of insoluble anhydrite after 150 hours. The hydrate water content of the solid increases slightly after contact with the solution and then reverses its trend to decrease to less than 1% after 40 hours contact time. The orthorhombic crystal structure of insoluble anhydrite was indicated by x-ray diffraction examination of the solid phase after 150 hours exposure at 95° C. Again this behavior is in strong contrast to that in water, in which, below the meta-stable equilibrium temperature of about 99° C., hydration to gypsum occurs but no further dehydration to anhydrite occurs, at least over periods of days.

β-Soluble Anhydrite. The solubility and hydration behavior in water of β-soluble anhydrite at the experimental temperatures of 85° C. and less was identical to that of β-hemihydrate (*7*), indicating that the hydration of the anhydrite to the hemihydrate is much faster than the hydration of β-hemihydrate to gypsum.

In 1*m* NaCl, at 25° to 45° C., β-soluble anhydrite again showed the same behavior—an initially high transient solubility followed by a drop to the solubility of gypsum and a solid composition corresponding to the dihydrate. At 65° C., the solute concentration remained constant and equal to the solubility of gypsum for a period of from 0.5 to 24 hours, but the composition of the solid phase slowly dropped from 18.0% H_2O at 0.5 hour to 16.4% H_2O after 120 hours (Figure 1, bottom). In contrast, when starting with β-hemihydrate, the solid composition stayed essentially constant at 20% H_2O for 24 hours. Figure 1, bottom, shows that at 75° C. the calcium sulfate concentration in contact with β-soluble $CaSO_4$ equaled the solubility of gypsum for about 20 hours and then slowly decreased. The solid phase slowly dropped from 12.4% H_2O after 6 hours to 2.3% H_2O at 117 hours and 0.72% H_2O at 246 hours. The conversion of β-soluble anhydrite (monoclinic) to insoluble anhydrite (orthorhombic) after 30 hours at 85° and 95° C. was again confirmed by x-ray diffraction examination.

In 0.25*m* NaCl solution, the approach of solute concentration to the solubility of insoluble anhydrite was more rapid at 85° and 95° C. with β-soluble anhydrite than with β-hemihydrate, and the brief hydration period of β-soluble anhydrite was less pronounced than for β-hemihydrate.

Insoluble Anhydrite. A previous study (*7*) showed that, after a rapid initial rate of solution, the calcium sulfate solute concentration continues to increase slowly over periods of days when insoluble anhydrite is contacted with pure water. The phenomenon was especially noticeable at temperatures of 65° C. and below, and the ultimate solute contents substantially exceeded those previously reported for anhydrite solubility. Even after 160 hours of contact with water at 85° C., the bound water content of the solid anhydrite, originally 0.0%, did not exceed 1%. X-ray diffraction studies of the solid after this period of contact indicated the presence only of the insoluble anhydrite modification, but the method was not sufficiently sensitive to detect 1% or less of another crystal form.

When insoluble anhydrite was contacted with 0.25*m* or 1.0*m* sodium chloride solution, a slight increase in calcium sulfate concentration from zero to about 0.5% also occurred over the period from 6 to 48 hours. The rate of increase is greater at the lower temperatures, but the effect is less pronounced than in water. Table II gives solubility data for anhydrite in water and in 0.25*m* and 1.0*m* NaCl over the temperature range of 35° to 85° C. The values reported are those extrapolated to zero time.

Summary of Solubilities. The solubilities of gypsum and insoluble anhydrite as a function of temperature in 0.25*m* and 1.0*m* aqueous NaCl are shown in Figure 2. With β-soluble hemihydrate and β-soluble anhydrite, the phase changes occurred too rapidly to establish these solubilities accurately by the present experimental technique. In 0.25*m* NaCl, solubilities of both calcium sulfate modifications are about twice that in pure water and in 1.0*m* NaCl, are about three times as great.

Bock (*1*) has reported that the transition temperature between gypsum and anhydrite decreases with increased sodium chloride content from a value of, for example, 42° C. in pure water to 40–41° C. in 1*m* NaCl and 25° C. in 4.3*m* NaCl. Within an experimental error of about 1° C., the authors' data show the transition temperature to be about 41° C. in water, about 40° C. in 0.25*m* NaCl, and 39° C. in 1*m* NaCl, in essential agreement with the values of Bock.

CORRELATION OF DATA

From the theory of thermodynamic properties of electrolytic solutions, the mean activity coefficient of a strong electrolyte can be expressed as (*4*)

$$\log \gamma_{AB} = - \frac{\frac{1}{\sum \nu_i} \sum \nu_i z_i^2 \frac{1.290 \times 10^6 (2\mu)^{1/2}}{(DT)^{3/2}}}{1 + a^0 \frac{35.56}{(DT)^{1/2}} (2\mu)^{1/2}} \quad (1)$$

where

D is the dielectric constant of water
T is the absolute temperature
μ is the ionic strength of the solution, $= \frac{1}{2}\sum m_i z_i^2$
a^0 is the ionic parameter in Angstrom units
ν is the number of ions of species i formed by one molecule of electrolyte
z is the valence of ion species i

According to this expression, the mean activity coefficent for calcium sulfate in water is

$$\log \gamma_{CaSO_4} = - \frac{[(7.296 \times 10^6)/(DT)^{3/2}] (\mu)^{1/2}}{1 + \frac{A}{(DT)^{1/2}} (\mu)^{1/2}} \quad (2)$$

where $A = a^0 \times 35.56 \times (2)^{1/2}$.

An equivalent expression can be written for the activity coefficient of calcium sulfate in a sodium chloride solution. The ratio of molalities of calcium sulfate in pure water and in the presence of cosolute with different ions becomes:

$$\log m'/m = \frac{[(7.296 \times 10^6)/(DT)^{3/2}] [(\mu')^{1/2} - (\mu)^{1/2}]}{1 + \frac{A}{(DT)^{1/2}} [(\mu')^{1/2} + (\mu)^{1/2}] + \frac{A^2}{DT} (\mu')^{1/2} (\mu)^{1/2}} \quad (3)$$

Table I. Solubility Data for Gypsum

Temperature, °C.	Temperature, °K.	D	$A/(DT)^{1/2}$
25	298	78.28	1.544
35	308	74.77	1.553
45	318	71.40	1.564
55	328	68.18	1.577
65	338	65.09	1.589
75	348	62.15	1.602
85	358	59.33	1.618
95	368	56.65	1.632

Temp., °C.	Molal Solubility $CaSO_4$	Molality NaCl	μ	γ	$K°$	$K°_{av.}$
25	0.0154	0	0.0616	0.430	43.9×10^{-6}	
	0.0288	0.25	0.3652	0.229	43.5×10^{-6}	
	0.0451	1.00	1.1804	0.147	44.0×10^{-6}	43.8×10^{-6}
35	0.0156	0	0.0624	0.421	43.1×10^{-6}	
	0.0292	0.25	0.3668	0.223	42.4×10^{-6}	
	0.0456	1.00	1.1824	0.143	42.5×10^{-6}	42.7×10^{-6}
45	0.0154	0	0.0616	0.415	40.8×10^{-6}	
	0.0291	0.25	0.3664	0.217	39.9×10^{-6}	
	0.0458	1.00	1.1832	0.138	39.9×10^{-6}	40.2×10^{-6}
65	0.0147	0	0.0588	0.406	35.6×10^{-6}	
	0.0286	0.25	0.3644	0.205	34.4×10^{-6}	
	0.0450	1.00	1.1800	0.129	33.7×10^{-6}	34.6×10^{-6}
85	0.0134	0	0.0536	0.402	29.0×10^{-6}	
	0.0268	0.25	0.3572	0.194	27.0×10^{-6}	
	0.0439	1.00	1.1756	0.118	26.8×10^{-6}	27.6×10^{-6}
95	0.0127	0	0.0508	0.398	25.5×10^{-6}	
	0.0262	0.25	0.3548	0.186	23.7×10^{-6}	
	0.0432	1.00	1.1728	0.113	23.8×10^{-6}	24.3×10^{-6}

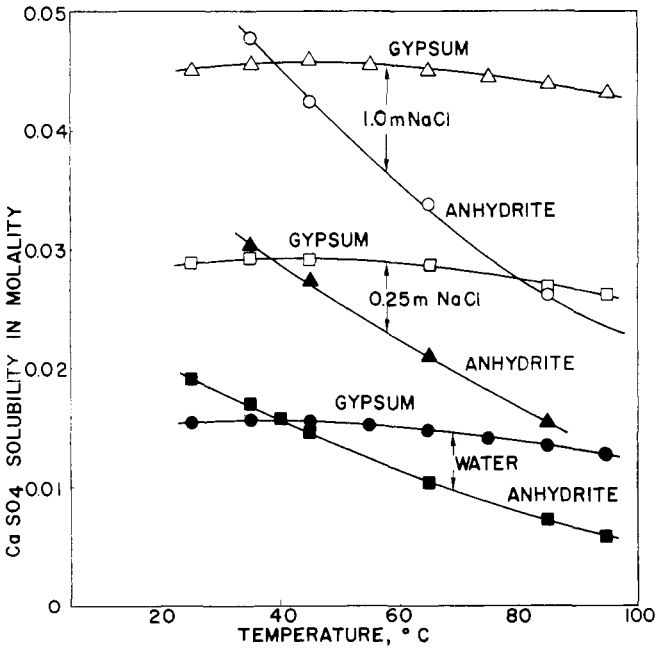

Figure 2. Solubilities of gypsum and anhydrite in water, 0.25*m* NaCl, and 1.0*m* NaCl

where μ' is the ionic strength of the solution containing cosolute.

The constant A contains the ionic parameter, a^0, the minimum distance to which ions, both positive and negative, can approach one another. Unfortunately, this parameter is not clearly established in mixtures of strong electrolytes, so that A becomes an adjustable constant, which was determined from our gypsum solubility measurements at 25° C. to have a value of 2.357×10^2. Up to an ionic strength of about one, the value of A is essentially constant in the present system, but at higher ionic strengths, it decreases with increased ionic strength for temperatures up to at least 60° C. The resultant value of $A/(DT)^{1/2}$ at 25° C. is 1.54, in good agreement with the value of 1.50 reported by Marshall, Slusher, and Jones (5). The constancy of the value of A over this range of ionic strengths was also brough out by the results of these authors.

The solubility product constant, $K°$, (or thermodynamic activity product) for calcium sulfate is

$$K° = m^2\gamma^2 \tag{4}$$

This neglects the relatively small correction for the activity of water when gypsum or hemihydrate is the saturating solid phase. For each solubility datum, the activity coefficient was determined from Equation 2 and the solubility product constant, $K°$, from Equation 4. Table I gives the results of these calculations for the temperature range of 25° to 95° C., and the average value of the solubility product constant, $K°$ at each temperature. There is relatively little scatter in the experimental results. If the measured solubilities are compared with those calculated from Equations 2 and 4, the average deviation is ±0.8%, and the maximum deviation is 2.4%.

Solubility product constants for insoluble anhydrite were determined by the same procedure used for gypsum. The experimental results and the calculations are summarized in Table II. The scatter in the results is moderately greater than is the case with gypsum. If measured solubilities are compared with those calculated from Equations 2 and 4 as above, the average deviation is ±2.7%, and the maximum deviation is 6.9%.

Table II. Solubility Data for Insoluble Anhydrite

Temp., °C.	Molal Solubility $CaSO_4$	Molality NaCl	μ	γ	$K°$	$K°_{av.}$
35	0.0170	0	0.0680	0.410	48.5×10^{-6}	
	0.0301	0.25	0.3704	0.222	44.8×10^{-6}	
	0.0478	1.00	1.1912	0.143	46.5×10^{-6}	46.6×10^{-6}
45	0.0147	0	0.0588	0.422	38.4×10^{-6}	
	0.0273	0.25	0.3592	0.219	35.7×10^{-6}	
	0.0425	1.00	1.0816	0.139	34.9×10^{-6}	36.3×10^{-6}
65	0.0103	0	0.0412	0.454	21.8×10^{-6}	
	0.0208	0.25	0.3332	0.212	19.5×10^{-6}	
	0.0337	1.00	1.1348	0.130	19.3×10^{-6}	20.2×10^{-6}
85	0.0072	0	0.0288	0.485	12.2×10^{-6}	
	0.0153	0.25	0.3112	0.204	9.7×10^{-6}	
	0.0261	1.00	1.1044	0.121	10.0×10^{-6}	10.6×10^{-6}

Table III. Comparison of Reported Solubility Data

Author	Ref.	Salt	Ionic Strength Range	Temp. Range, °C.	Av. Dev. from Eq. 3, %
Bock	(1)	NaCl	0–1.1	25–50	2.6
Denman	(3)	NaCl	0–0.82	25	1.4
		KCl	0–0.08	25	0.3
		$MgCl_2$	0–0.14	25	0.8
		NaCl	0–0.27	81–91	3.0
Marshall	(5)	NaCl	0–1.08	40–60	1.1
Shternina	(8)	NaCl	0–1.05	25	2.9

Figure 3 compares solubility product constants obtained by Marshall, Slusher, and Jones (5) with the authors' data. The agreement is generally excellent, although the two data points in their work for insoluble anhydrite at 40° and 60° C. are higher than the present ones by about 10%. This may reflect at least in part the gradual increase of solute concentration with time which occurs in contact with insoluble anhydrite. The authors' values are those extrapolated back to zero time whereas those of Marshall and coworkers apparently were developed from solute concentrations obtained after various contact times.

Data in the literature on the solubility of gypsum and anhydrite in sodium chloride, potassium chloride, and magnesium chloride solutions were also compared with values calculated from Equation 3. Up to an ionic strength of about one, the calculated and experimental values showed satisfactory agreement, as shown in Table III. Above an ionic strength of about one, the calculated solubilities exceeded the experimental values. From all available data, a correction factor was calculated by the least squares method and is plotted as a function of the square root of ionic strength in Figure 4. This expression cannot be expected to apply for ionic strengths higher than those used in developing the correlation. Thus the data of Morozova and Firsova (6) on the solubility of gypsum in mixtures of sodium chloride and magnesium chloride are substantially different than solubilities predicted above, presumably owing to the high $MgCl_2$ concentrations in their studies. By dividing the molality of gypsum or anhydrite as calculated from Equation 3 by this factor, the correct solubility can be obtained—i.e., $m_{corr.} = m/f$. The correction factor values above μ of about 1.35 can be expressed by the empirical equation.

$$\log f = 0.0034 - 0.0685\,\mu^{1/2} + 0.0590\,\mu \qquad (5)$$

with a standard deviation of the calculated solubility of 2.3% at $\mu = 1.0$, 3.5% at $\mu = 1.5$, 4.6% at $\mu = 2.0$, and 5.8% at

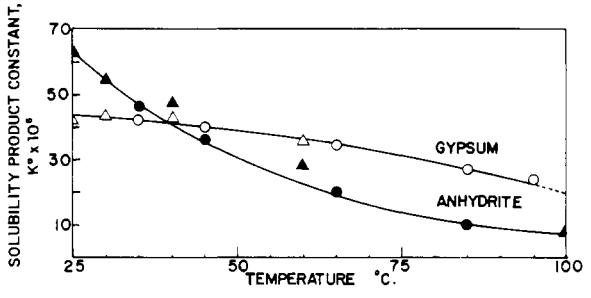

Figure 3. Solubility product constants of gypsum and anhydrite
▲△ Data of Marshall *et al.* (5)
●○ Present data

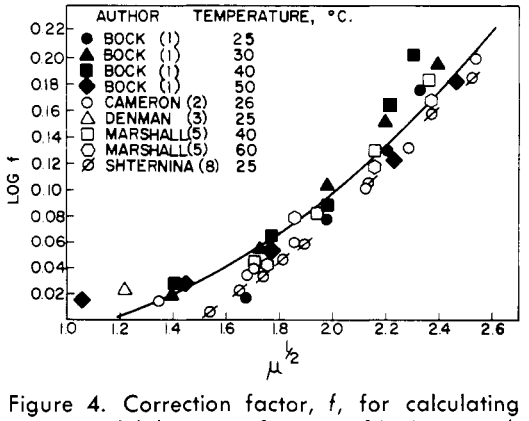

Figure 4. Correction factor, f, for calculating gypsum solubilities as a function of ionic strength

μ = 2.5. No definite trend in the change of the correction factor with temperature could be detected.

CALCULATION OF SOLUBILITIES

The solubility of gypsum or of insoluble anhydrite can be calculated by Equation 4, using the solubility product constant values of Tables I and II, and determining the activity coefficients by Equation 2. Above an ionic strength of 1.0, the calculated solubility must be corrected by a factor given by Equation 5.

ACKNOWLEDGMENT

Solute concentration measurements and solid phase analyses were made by J.P. DeMonico. X-ray diffraction studies were made by R.R. Ferguson in the Dayton Laboratories of Monsanto Research Corp. This work was sponsored by a contract from the Office of Saline Water, U. S. Department of the Interior. We also acknowledge the careful and helpful review of the original manuscript by W.L. Marshall.

LITERATURE CITED

(1) Bock, E., *Can. J. Chem.* **39**, 1746 (1961).
(2) Cameron, F.K., *J. Phys. Chem.* **5**, 556 (1901).
(3) Denman, W.L., *Ind. Eng. Chem.* **53**, 817 (1961).
(4) Harned, H.S., Owen, B.B., "The Physical Chemistry of Electrolytic Solutions," pp. 59-66 Reinhold, New York, 1958.
(5) Marshall, W.L., Slusher, R., Jones, E.V., J. CHEM. ENG. DATA **9**, 187 (1964).
(6) Morozova, A.I., Firsova, G.N., *Nauch. Trudy Novocherkassk. Politekh. Inst. Im. S. Ordzhonikidze* **27**, 151 (1951).
(7) Power, W.H., Fabuss, B.M., Satterfield, C.N., J. CHEM. ENG. DATA **9**, 437 (1964).
(8) Shternina, E.G., *Izv. Sektora Fiz. Kim. Anal. Inst. Obshchei Neorg. Khim. Akad. Nauk SSSR* **17**, 351 (1949).

RECEIVED for review December 2, 1964. Accepted January 12, 1966.

Critical Temperatures and Critical Pressures of the Ethane–*n*-Pentane System

OKAN EKINER and GEORGE THODOS
Northwestern University, Evanston, Ill.

The critical temperatures and critical pressures of three ethane–*n*-pentane mixtures were established experimentally and were used to obtain the dependence of these critical values on composition. A visual *P-V-T* cell of the mercury piston type was used to determine these critical constants for binary mixtures, each having an ethane content of 0.562, 0.766, and 0.888 mole fraction. To accomplish this objective, the vapor-liquid phase behavior of each mixture was determined and utilized to obtain the pressure-temperature relationships having constant liquid volume per cent lines as parameters. All of these relationships converged to the critical point of each mixture. The resulting critical temperature-composition and critical pressure-composition relationships have been compared with the corresponding critical values reported in the literature for this system.

CONTINUING interest in the accurate determination of the critical temperatures and critical pressures of hydrocarbon mixtures requires that these critical properties be well established for binary systems. To assist in this direction, the critical behavior of the ethane–*n*-pentane system was investigated by determining the critical temperatures and critical pressures of three binary mixtures of these components.

These critical values were experimentally determined using a visual *P-V-T* cell in which mercury was used as the displacing fluids. The details of the experimental equipment and procedure used are described at length elsewhere (*1*). The hydrocarbons used in this study were of research grade and were obtained from the Phillips Petroleum Co. The purity of the ethane was claimed to be 99.96% while that of *n*-pentane was claimed to be 99.84%. These components were first introduced into a charging cell preceding the visual *P-V-T* cell where they were solidified with liquid nitrogen and then were exposed to vacuum. In order to ensure complete removal of any noncondensables, the charging cell and its contents were warmed to room temperature, were then again solidified with liquid nitrogen and evacuated. This procedure was repeated at least three times to ensure complete removal of any noncondensables in the hydrocarbon mixture.

ESTABLISHMENT OF CRITICAL POINT

A mixture of ethane and *n*-pentane was charged into the *P-V-T* cell, which was surrounded by an air bath whose temperature could be accurately regulated. The volume of the liquid and vapor phases existing in equilibrium with each other could be observed at all times visually with a cathetometer. The *P-V-T* cell was supported on a trunion and was rocked to hasten the establishment of equilibrium of its contents. The position of the vapor-liquid meniscus and the mercury-liquid meniscus existing at equilibrium conditions provided the necessary information to establish the liquid volume per cent prevailing at the temperature and pressure conditions within the cell. By holding the temperature constant, mercury was introduced into the cell to increase the pressure of the system. This approach was continued until a single homogeneous phase was obtained. Depending on the temperature of the system, this homogeneous phase could be either all liquid or all vapor. This procedure was repeated using different constant temperatures in the vicinity of the critical temperature of the mixture. Figure 1 presents the resulting pressure *vs.* liquid volume per cent isotherms for a mixture of 0.562 mole fraction ethane. These isotherms range from 256.8 to 286.1° F. and exhibit a complete reversal at 277.5, 281.9, and 286.1° F.,